CHEMISTRY
A EUROPEAN JOURNAL

Supporting Information

Spontaneous Discrimination of Polycyclic Aromatic Hydrocarbon (PAH) Enantiomers on a Metal Surface

Gonzalo Otero,[a] Giulio Biddau,[b] Taisuke Ozaki,[c] Berta Gómez-Lor,[a] Javier Méndez,[a] Rubén Pérez,*[b] and Jose Angel Martín-Gago*[a]

chem_201002079_sm_miscellaneous_information.pdf

Supplementary Information

1. Experimental details

The syntheses of $C_{60}H_{30}$ was performed in just two steps starting from 10,15-dihydro-5H-diindeno[1,2-a:1',2'-c] fluorene (truxene) as previously reported in ref. [1]. A description of the calculated molecular structure in vacuum can be found in ref. [2]. The experiments were performed *in situ* in an ultra high vacuum (UHV) system with a base pressure of $1x10^{-10}$ mbar equipped with Auger electron spectroscopy, low-energy electron diffraction optics, STM at room temperature (300 K) and thermal programmed desorption (TPD).

The molecules were sublimated *in situ* by thermal evaporation (660 K) and deposited on a previously atomically cleaned Pt(111) surface. The temperature of the substrate during the deposition was 300 K. Standard cycles of sputtering and annealing (at 1200 K, 20 min.) were performed to clean the platinum surface. The first annealing cycle was performed in an oxygen atmosphere ($P=1.10^{-5}$ mbar) and subsequent on UHV with a maximum pressure of $7x10^{-10}$ mbar.

We have studied by room temperature STM images the adsorption site and population of the different species. The images were recorded in topographic mode, using typical values for the tunnel current of 0.25 nA and bias voltages ranging from -2000mV to -50mV and 50mV to 2000mV. Images were analyzed with the WsxM software [3].

2. Experimental determination of the angle formed between the molecules and the crystallographic surface directions.

It is generally accepted that a STM image of an organic molecule reflects the charge density associated with the molecular orbitals in an energy range determined by the bias voltage and the Fermi level. Hence, a STM image cannot always be directly overlaid to a molecular model. We discuss hereafter the methodology we have followed to relate the STM images of the adsorbed $C_{60}H_{30}$ molecules with the real position of the molecule.

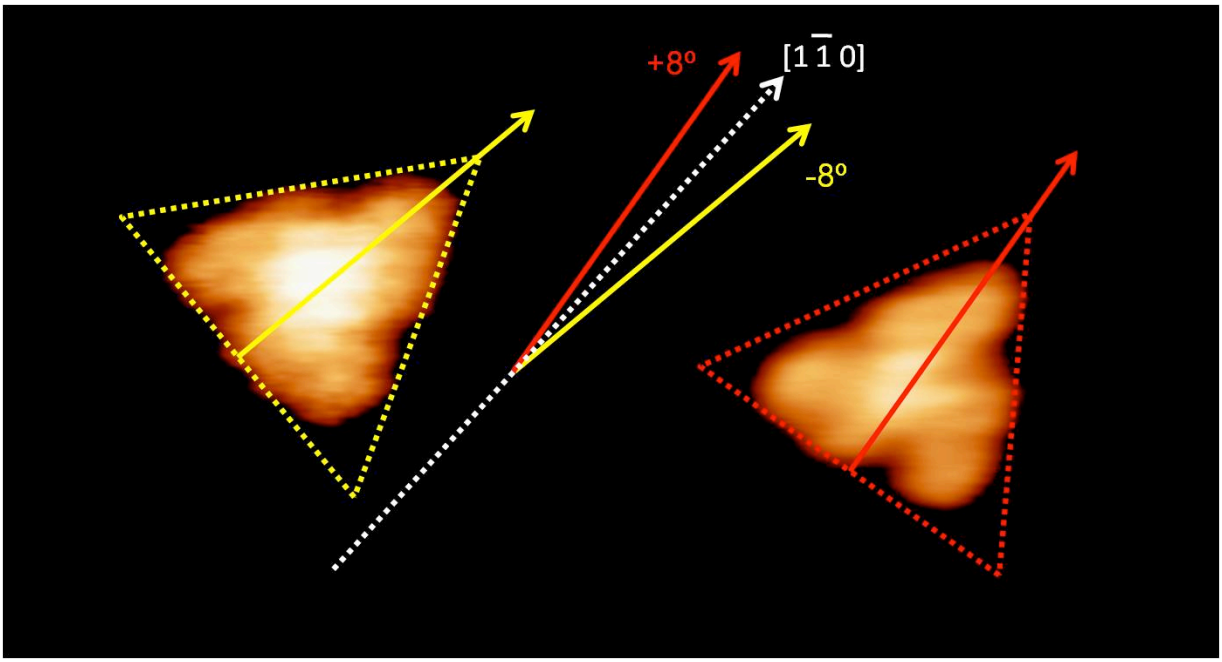

Fig. S1.- *STM images showing two $C_{60}H_{30}$ molecules adsorbed on the surface with different chiral configurations.*

The first step consists of determining the [1-10] surface direction on the STM images. i.e., to draw the white dashed arrow in Fig. S1. We have obtained atomic resolution images on the Pt(111) surface but, unfortunately, never after dosing the molecules. We have determined the surface crystallographic directions in our experimental set-up by analysing the LEED pattern, and crosschecking it with the running monoatomic step-edges observed in many STM images. Combining all this information we are able to determine the [1-10] surface direction with a precision better than 2 deg.

The second step consists of determining the angle between molecules owing different chiralities, as the ones shown in Fig. S1. This can be done easily, just enclosing every one of the images within a triangle and drawing the height of this triangle, as it is also indicated in Fig. S1. For instance, in this figure the height of the triangles enclosing the two imaged molecules are split by 16 ± 3 deg. The error value corresponds to the standard deviation obtained after statistically averaging over hundreds of molecules in several images with scanned areas about 50 x 50 nm^2, as the shown in Fig. 2 (paper) and Fig. S2. The main source of the statistical error is the experimental drift. In this determination the crystallographic direction of the Pt lies in the middle. Interestingly, the molecular shape imaged by STM does not change with the bias voltage.

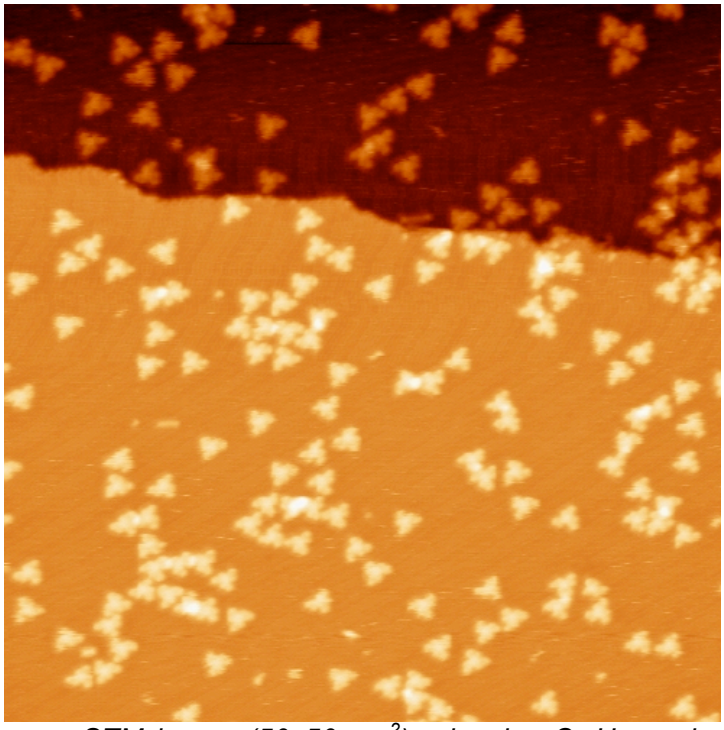

Fig. S2.- *Long range STM image (50x50 nm^2) showing $C_{60}H_{30}$ molecules adsorbed on the Pt(111) surface. Typical bias voltages and tunnel currents are 750 mV and 0.2 nA, respectively.*

The third step is the most intricate one, because it involves the correlation between the STM image and the real structure of the molecule, as discussed at the beginning of the section. This correlation can be obtained throughout DFT calculations that could help us to elucidate the local density of states. Fig. S3-a shows the molecular structure of a $C_{60}H_{30}$ molecule adsorbed on Pt(111) in the most energetically favourable left-configuration obtained from our *ab-initio* calculations. Fig S3-b and S4 display a simulated STM image for that configuration. We have used a simple Tersoff-Hamann approximation based on the calculated local density of states $\rho(r,E)$ integrated in the energy range (E_F – 1V, E_F). In this figure the isosurface corresponds to a constant value of the LDOS of $4x10^{-4}$ Å^{-3}, that would provide a current and a corrugation height of 0.7 Å, close to the experimental values [4]. In the centre and in the C rings close to the pentagons of the molecule, the LDOS is larger than in the peripheral C-rings. In particular, we obtain the lowest value for the LDOS in the outermost hexagonal carbon rings (encircled with a white line on Fig. S3). Thus we can separate the LDOS in two well-differentiated parts: higher values (central part of the molecule, in Fig. S3-b) and lower values (white circles at the peripheral carbon-rings of the molecules). Fig. S4 shows the result of the Tersoff-Hamann calculations in 3D perspective to provide a direct view of the fact that the central part of the molecule appears enhanced with respect to the peripheral carbon rings.

In Fig. S3-c we have superimposed the combination of circles and triangles obtained by our calculations on the experimental STM image. It is clear that molecules resolved by STM images show enhanced intensity in the molecular region corresponding to centre of the molecule, but reduced one on the most peripheral carbon rings. This indicates that the outermost hexagonal rings are faintly imaged by STM due to a lower DOS. The difference between the real molecular structure and the

STM shape has to be taken into account to elucidate the existent molecular orientation with respect to the crystallographic directions (Fig. S5).

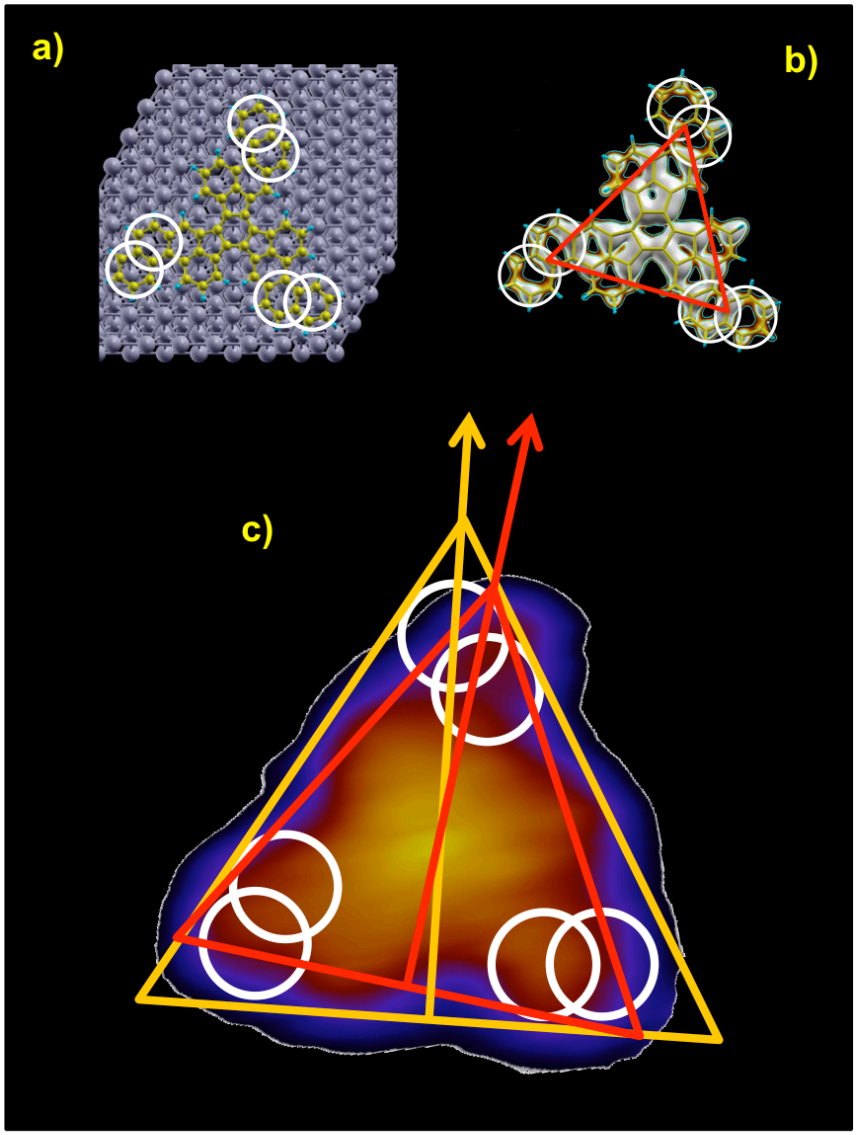

Fig. S3. *Angle between the adsorbed molecules and the crystallographic surface directions. a) Optimized molecular structure with ab initio calculations for the most energetically favourable left-configuration of the $C_{60}H_{30}$ molecule on Pt(111). b) Simulated STM image for (a) (see Fig. S4 for details). c) Experimental image obtained with STM for the same configuration. STM images do not show the outermost hexagonal-carbon rings of the molecule (white circles), and consequently a correction factor of 9º has to be added to the experimentally determined value of Fig. S1.*

The red triangle enclosing the molecule in the figure S3-c is the same discussed in the second step (see Fig. S1), which present its height (red arrow) rotated 8º with respect the [1-10] surface crystallographic direction. However, the fact that STM not show the outermost carbon ring introduces

a systematic error in the determination of the angle between the STM image and the surface. To correct this error we have to consider the real structure of the molecule that we have derived by *ab-initio* calculations, i.e., we have to include the position of the external white circles for constructing our corrected triangle (in orange in the Fig. S3-c). As we can see in Fig. S3-c the orange triangle is rotated 9º in the counter-clockwise direction with respect to the red triangle. Consequently the orientation of the molecule, determined throughout STM images will be (8º + 9º) = 17º with respect to the [1-10] crystallographic direction. The discrimination process is schematically represented in Fig. S5. Similarly, for the case of the right-configuration, we have to add 9º towards the opposite direction, and therefore the molecule will form -17º with the crystallographic direction. A possible source of error for this determination could come by thermal drift inducing different sizes of the STM images, which could alter the position of the end of the molecule. However, the incertitude drawing the orange triangle in the Fig. S3-c is smaller than 3º. Consequently, we can safely determine the angular difference between molecules adsorbed in left and right – configurations to be 34 ± 6 deg.

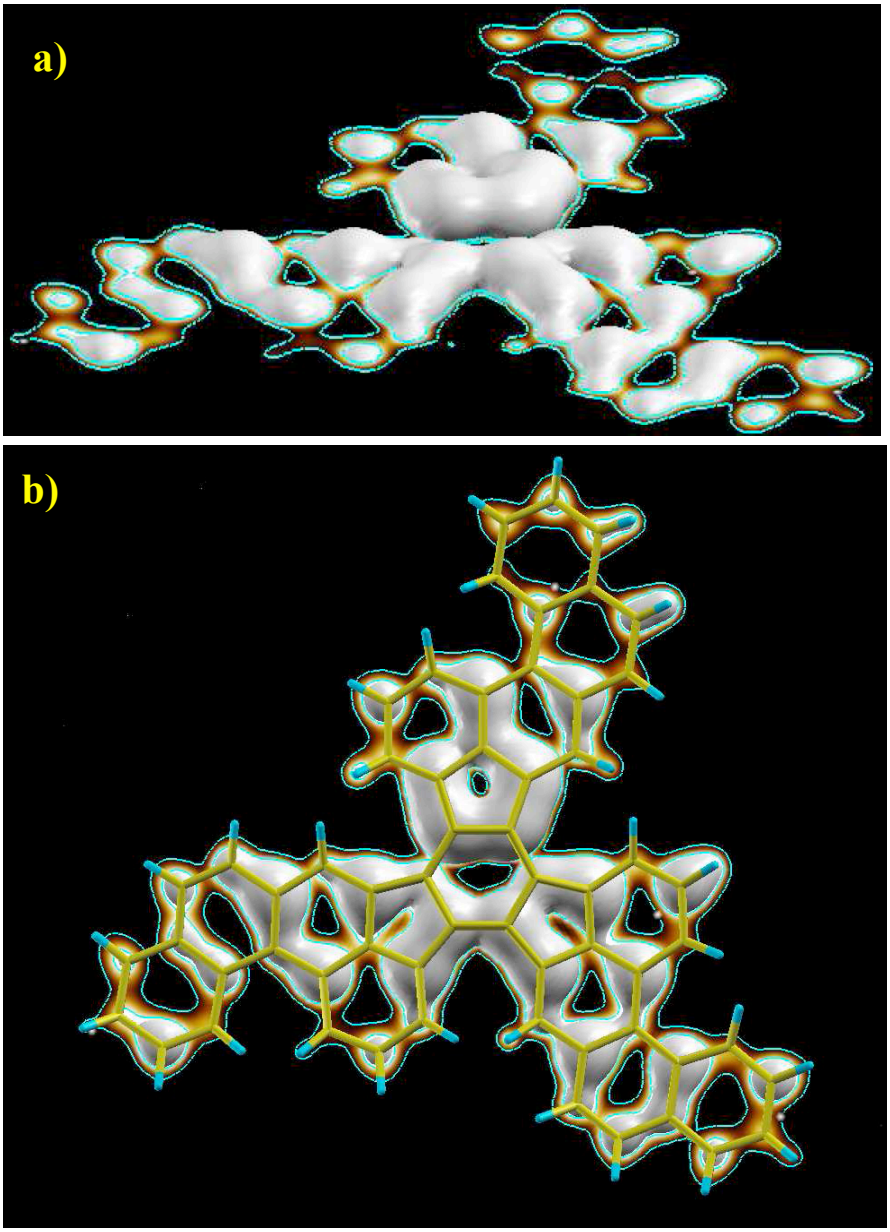

Fig. S4. *Simulated STM image for the configuration in Fig. S3-a, using the Tersoff-Hamman approach and the experimental operating conditions (bias = -1 V). The local density of states $\rho(r,E)$ has been integrated in the range (E_F – 1V, E_F). The grey surface represents a constant value of $4x10^{-4}$ $Å^{-3}$, that corresponds to a current close the experimental one [4]. (a) top view, highlighting the areas of the molecule that dominate the STM contrast (b) side view (perspective). The STM tip follows the isosurface, resulting in a corrugation (difference in height between the central area and the outer rings) of 0.7 Å*

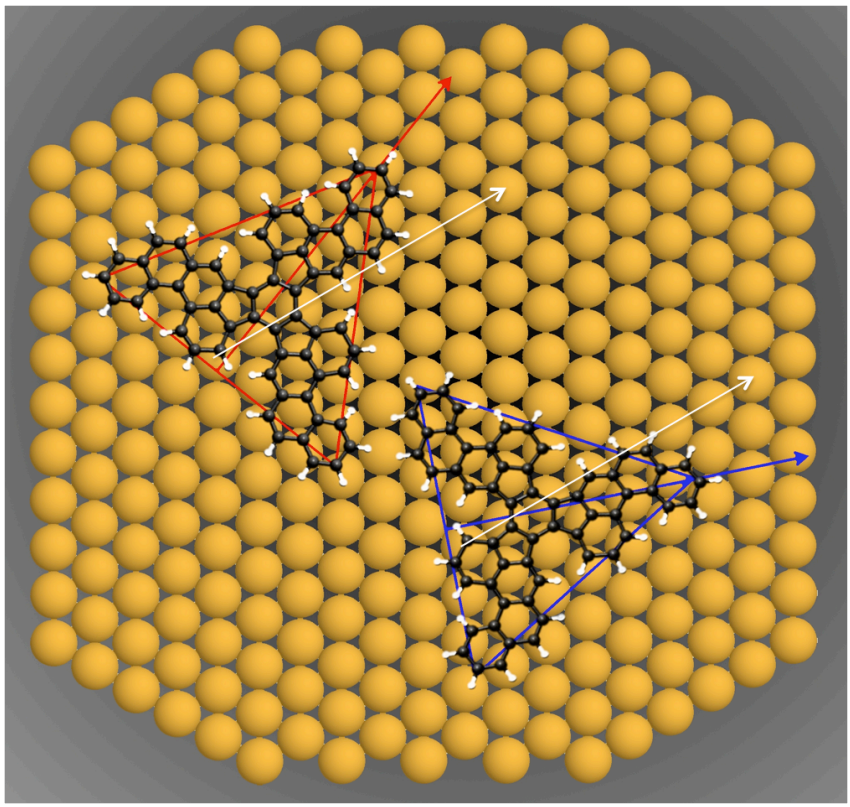

Fig. S5.- *Schematical representation of the enantiomeric discrimination process. Molecules adsorbed right or left are adsorbed at -17 or +17 degrees with respect to the [1-10] surface crystallographic direction (white arrow).*

3. Computational methods: Basis set and Exchange-correlation functional.

DFT calculations have been performed with the OPENMX [5] code, that solves the Kohn-Sham equations in a local orbital basis. This basis is formed by a collection of strictly localized pseudo-atomic orbitals (PAOs) centered on atomic sites [6,7]. These PAOs are the solutions of the atomic Schrodinger equation with an additional confinement potential that enforces the wave-function to go to zero at the cutoff radius. In the calculations reported here, we have used an optimized basis defined by C5.0-s2p3 (C5.0-s52p53d51), H4.5-s1 (H4.5-s21) and Pt7.0-s2p2d2, where the notation indicates the atomic specie, the cutoff radius (in Bohr) and the number of orbitals with a l=s,p,d symmetry included in the basis. The values in parenthesis refer to the original set of primitive orbitals to which optimization [6,7] was applied (e.g. p53 means that three optimal p orbitals have been generated from five p orbitals). Our basis set for C and H has been optimized to reproduce the results of converged plane-wave calculations (using VASP) for (1) the C-C, C-H and C-Pt bond distances in a wide range of carbon rich materials (CRMs) including hydrocarbons (methane, acetylene, ethylene, ethane), benzene, pyridine, fullerenes, azafullerenes and graphene; and (2) total energy differences among a large number of configurations in hydrocarbons including aromatic rings with very different

compositions C_xH_y that are relevant in the process of cyclyzation of dehidrogenated PAHs to form closed fullerenes. No optimization was performed for the Pt basis set.

There is an on-going debate in the literature concerning the best functional to describe the interaction of aromatic molecules with metal surfaces. As LDA is known to overestimate the bonding energies, GGA functionals (PBE in our case) are a priori the best option. However, GGA calculations give molecule-surface distances far larger than the ones determined from experiments for certain well studied cases like PTCDA on Ag(111). When vdW corrections are added to the GGA functional, the resulting structures and total energies tend to be quite close to the LDA results. As our conclusions regarding the preferential orientation of the prochiral molecule $C_{60}H_{30}$ rely on marked differences among adsorption configurations, we have explored in detail their dependence on the approximation used for the exchange-correlation potential in a simple case: the adsorption of benzene on Pt(111) using a 3x3 surface unit cell using both VASP and OPENMX. In the case of VASP, we have reproduced the results of Morin *et al* [8] for the Perdew-Wang-91 (PW91) GGA functional, and calculated the same structures with PBE and LDA. Our calculations confirm that although absolute adsorption energies are quite different for the LDA and GGA approximations, both functionals do provide the same energy differences among the various relevant configurations. This same study shows that while absolute adsorption energies are also quite sensitive to the number of layers in the metal slab, energy differences among the different adsorption configurations are converged (with an error less than 5%) on a three-layer slab.

4. Making contact with the STM images: Internal distortions and Density of state calculations.

The ground state configuration for adsorption shows marked differences in height with respect to the surface for the various rings in the molecule: the carbon atoms on the central hexagon have relaxed outwards and are on average 0.41 Å higher than the atoms on the outer hexagons (average height: 2.12 Å) as shown in the side view at the bottom of figure 3. These height differences correlate with the weight of the density of states (DOS) associated to the π orbitals in the relevant energy range around the Fermi level. Figure S6.1 displays the sum of DOS projected on the p_z-orbitals for the central ring, one of the internal hexagons and the outermost benzene-like ring. The comparison with the sum of the total DOS projected on those atoms clearly shows that the states around the Fermi level are essentially of p_z character. The DOS is dominated in the [-1,1] eV energy range by the central ring, while the contribution of the outer rings, more strongly bonded and closer to the surface as we move away from the center, is significantly depleted. The combination of these geometrical and electronic effects explain the main features of the STM image for these molecules: the clear maxima around the central hexagon and the pentagons, and the missing outermost rings in each of the wings, with an apparent corrugation of 0.7 Å for the typical STM operation conditions.

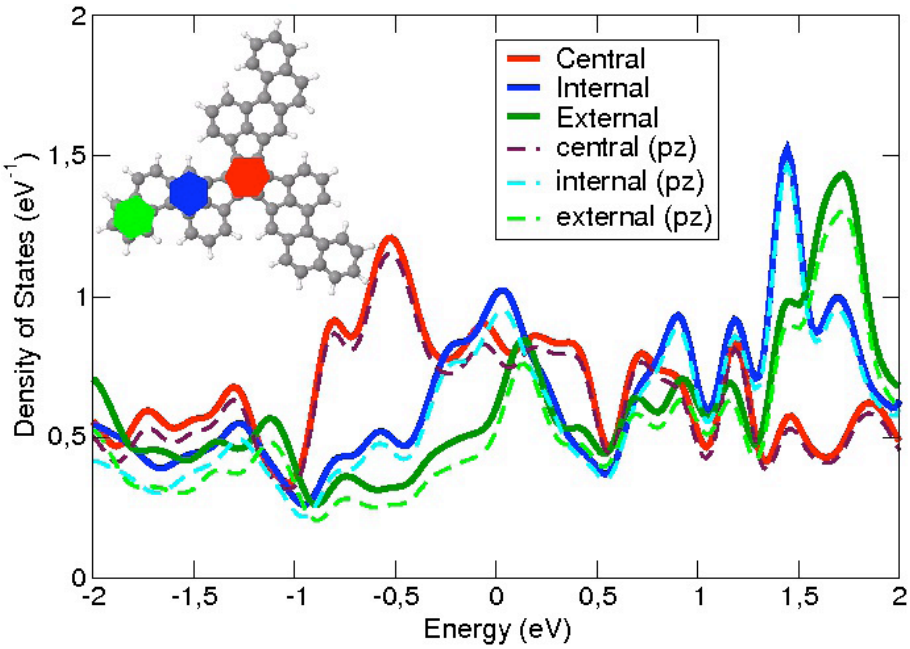

Fig. S6. *Density of States (DOS) in a range of [-2,+2] eV around the Fermi level for the ground state configuration for the adsorption of $C_{60}H_{30}$ on Pt(111). Thick lines represent the sum of the DOS projected on all of the carbon atoms for the central ring, one of the internal hexagons and the outermost benzene-like ring in one of the molecular wings (see inset). Dashed lines display the sum of the contribution of the p_z-orbitals on the same atoms. This comparison clearly shows that the states around the Fermi level are essentially of p_z character and are dominated by the central and internal rings.*

5. On the STM contrast between enantiomers in fig. 2 (or S1).

The contrast of the STM images included in figure 2, and particularly that of the inset (fig. S1 in the supp. Information) seems to present different contrast for every enantiomer. Contrast in a STM image is complex, because it strongly depends on the curvature radius of the tip or angle of scanning at this specific surface position, and the final appearance can be affected by the choice of a particular colour scale or pallet. The images referred reflect these inconveniences. However, in spite of the different visual appearance, the topography of both images is quantitatively very close: according to our measurements the difference is contrast-height of this image is smaller than 0.08 Å (less than 5% of the total height), a value completely negligible, albeit visible, with the colour scale chosen to emphasize the internal contrast inside the molecules. Nevertheless and more importantly, performing a statistical evaluation averaging on hundreds of molecules, all enantiomers present the same height and we do not have observed any particular trend in the STM contrast.

References

[1] B. Gómez-Lor, O. de Frutos, A. M. Echavarren, *Chem. Commun.* **1999**, 2431-2432.

[2] G. Otero, G. Biddau, C. Sánchez-Sánchez, R. Caillard, M. F. López, C. Rogero, F. J. Palomares, N. Cabello, M. A. Basanta, J. Ortega, J. Méndez, A. M. Echavarren, R. Pérez, B. Gómez-Lor, J. A. Martín-Gago, *Nature* **2008**, *454*, 865-868.

[3] I. Horcas, R. Fernández, J. M. Gómez-Rodríguez, J. Colchero, J. Gómez-Herrero, A. M. Baro, *Rev. Sci. Instrum.* **2007**, *78*, 013705 1-8.

[4] W. A. Hofer, A. S. Foster and A. L. Shluger, *Rev. Mod. Phys,* **2003**,*75*, 1287-1331.

[5] The code, OPENMX, pseudoatomic basis functions, and pseudopotentials are available on the web site (http://www.openmx-square.org/).

[6] T. Ozaki, *Phys. Rev. B*, **2003**, *67*, 155108 1-5.

[7] T. Ozaki, H. Kino, *Phys. Rev. B*, **2004**, *69*, 19513 1-19.

[8] C. Morin, D. Simon, P. Sautet. *J. Phys. Chem. B*, **2003**, *107*, 2995-3002.